

## Synthesis and characterization of silver-silica heterogeneous nanocomposite particles by an alcohol reducing method

Chang Young Kim and Sung-Chul Yi\*

Department of Chemical Engineering, Hanyang University, Seoul 133-791, Republic of Korea

We have used an alcohol reducing method of silver nitrate to prepare heterogeneous silver-silica nanocomposite particles with thiol and amino groups serving to bind the Ag nanoparticles to the surfaces of the SiO<sub>2</sub> nanoparticles. We examined products of these reductions using transmission electron microscopy and UV-vis. spectroscopy. The SiO<sub>2</sub> nanoparticles had diameters ranging from 70 to 90 nm; the Ag nanoparticles that formed on the surfaces of the SiO<sub>2</sub> nanoparticles had an average size of ca. 15 nm. The dimensions of the Ag nanoparticles on the SiO<sub>2</sub> surface were influenced by the molecular weight and concentration of polyvinylpyrrolidone (PVP) added to the reaction medium. In addition, the functional groups present on the surfaces of the SiO<sub>2</sub> nanoparticles had a profound influence on the coverage by Ag nanoparticles. When NH<sub>2</sub> groups were present on the surfaces of the treated SiO<sub>2</sub> nanoparticles, the sizes of the deposited Ag nanoparticles increased upon increasing the PVP concentration; in contrast, increasing the molecular weight of the PVP decreased the average size of these Ag nanoparticles. The Ag-SiO<sub>2</sub> nanocomposite prepared from SH-functionalized SiO<sub>2</sub> nanoparticles exhibited different behavior.

**Key words:** Silver-silica heterogeneous nanocomposite, Functionalizing agent, Thiol, amino, PVP.

### Introduction

Heterogeneous nanocomposite materials, such as gold-platinum, gold-palladium, silver-silica, and gold-titania, have been studied widely in recent years [1-5] because their catalytic properties differ dramatically from those of their single components. For example, the absorbance of metals coated on photocatalysts can be tuned selectively to any wavelength across the visible and infrared regions of the spectrum simply by adjusting the ratio of the size of the dielectric core to the thickness of the metal overlayer [6, 7]. In addition, Au/Pt composite nanomaterials exhibit a more efficient catalytic activity than do monodisperse Pt nanoparticles for both the hydrogenation of olefins and the visible-light-induced generation of H<sub>2</sub> from water [8].

In general, these types of nanocomposite structures have been fabricated by depositing nanoscale metal particles onto dielectric spheres. In particular, metal-coated SiO<sub>2</sub> surfaces have been fabricated using such approaches as electroless deposition [9], seed plating [10], surface functionalization [11], sputtering [12], layer-by-layer processing [13], and sonochemical deposition [14]. These SiO<sub>2</sub>-coating procedures are usually complex because they involve multi-step processes that make it difficult to obtain dense, uniform nanoscale metal layers of high purity. Several problems arise when immobilizing metal nanoparticles onto SiO<sub>2</sub> surfaces, including incomplete coverage, rough surfaces, and non-

uniformity of size and composition. Therefore, simple and controllable processes must be developed if these materials are to find industrial applications.

Silver is a widely used metal for the deposition of nanoparticles onto SiO<sub>2</sub> substrates [15-17]. The typical method comprises three steps: fabrication of SiO<sub>2</sub> microspheres, surface functionalization of the SiO<sub>2</sub> substrates with silane coupling agents, and deposition of preformed Ag nanoparticles onto the functionalized silica substrates through simple mixing. This process is not suitable, however, for forming a dense coverage of Ag on the SiO<sub>2</sub> substrates. Several effective metal particle adsorbents have been prepared through the immobilization of thiol ligands on the surfaces of silica gel [18, 19], clays [20, 21], polymers [22], and mesoporous silica [23]. The effectiveness of these materials in binding metal particles arises from forming complexes between the ligand and the metal, with the specificity of a particular ligand towards a target metal ion resulting from conventional acid-base interactions between the two. Although some of these thiol-functionalized adsorbents can form specific interactions with soft Lewis acids (such as Au<sup>+</sup>, Pd<sup>2+</sup>, and Ag<sup>+</sup>) [18-21], the selectivities of these materials are usually unremarkable because many metals have the ability to bind with thiol ligands. In a detailed study of the three-step fabrication method [24, 25], Halas and co-workers reported that surface functionalization of SiO<sub>2</sub> substrates with different terminal groups had a significant influence on the Ag coverage. Hydrophilic units, such as amino (NH<sub>2</sub>) and mercapto (SH) groups, promoted the attachment of Ag nanoparticles, whereas hydrophobic units, such as methyl (CH<sub>3</sub>) and diphenylphosphine (PPh<sub>2</sub>)

\*Corresponding author:  
Tel : +82-2-2220-0481  
Fax: +82-2-2298-5147  
E-mail: scyi@hanyang.ac.kr

groups, inhibited their attachment.

In this paper, we report a simple and rapid method using a silane coupling agent, an alcohol reducing method, and polyvinylpyrrolidone (PVP) as an additive for the preparation of heterogeneous Ag-SiO<sub>2</sub> nanocomposite particles. We studied the influence of (i) the molecular weight and concentration of PVP and (ii) the nature of the surface functional groups on the immobilization of the Ag nanoparticles onto SiO<sub>2</sub> surfaces. We used transmission electron microscopy (TEM) and UV-vis spectroscopy to characterize the resulting composite particles.

## Experimental

### Materials

Colloidal silica (21 wt%, SS-SOL 3080, ShinHeung Silicate, 70-90 nm) was used to prepare the SiO<sub>2</sub> nanoparticles. Absolute ethanol (HPLC grade 99.9%, Duksan Pure Chemical Company, Korea) was used as the solvent. 3-Mercaptopropyl trimethoxysilane (MPTMS) and 3-aminopropyltrimethoxysilane (APTMS) were purchased from Sigma-Aldrich (97%). Silver nitrate (99%, Junsei Chemical Co.) was used as a silver ion source. Polyvinylpyrrolidone polymers (PVP, Junsei Chemical Co.) having molecular weights of 10,000, 29,000, 40,000 and 58,000 were used as nucleation-promoting agents and stabilizers for the heterogeneous Ag-SiO<sub>2</sub> nanoparticles.

### Characterization

A Jeol JEM-2000EX II transmission electron microscope was used to investigate the formation and morphological properties of the Ag-SiO<sub>2</sub> nanocomposite particles. Each specimen for TEM analysis was prepared as follows: a drop of a diluted solution of the colloidal sample in ethanol was placed on a TEM grid (a copper grid pre-coated with amorphous carbon), which was then dried in an oven at 40 °C for 24 h prior to observation.

UV-Vis absorption spectra were recorded at room

temperature using a UV-1650PC spectrometer (Simadzu, Japan) over the wavelength range from 300 to 600 nm using a glass cuvette having an optical path length of 1 cm. Samples were diluted to a concentration of 20 ppm in ethanol.

### Synthesis and functionalization of silica substrates

SH and NH<sub>2</sub> functionalization of the surfaces of SiO<sub>2</sub> nanoparticles were performed using procedures similar to those described by Philipse and Vrij [17]. The colloidal SiO<sub>2</sub> was mixed with absolute ethanol under mild stirring. After 1 h, MPTMS or APTMS was added into the solution, which was then stirred gently for 6 h. The reaction mixture was centrifuged at 3,000 rpm for 30 minutes to separate the SiO<sub>2</sub> nanoparticles functionalized with SH or NH<sub>2</sub> groups. The separated nanoparticles were washed with ethanol (to remove any unreacted reagents) and collected.

### Preparation of heterogeneous Ag-SiO<sub>2</sub> nanocomposites

To immobilize the Ag nanoparticles onto the SiO<sub>2</sub> surfaces modified with SH or NH<sub>2</sub> groups, an alcohol reducing method was employed. The composition for each set of experimental conditions is indicated in Table 1. The Ag concentration was fixed at 0.1% (w/v) throughout these experiments. A typical procedure is described. SiO<sub>2</sub> particles functionalized with SH or NH<sub>2</sub> groups were dispersed in ethanol under sonication. PVP was dissolved in the mixture while gently stirring to prevent distortion of the polymer chain. After complete dissolution of the PVP, AgNO<sub>3</sub> was added to the solution, which was then heated with stirring at 78 °C for 5 h.

## Results and Discussion

We functionalized the surfaces of SiO<sub>2</sub> nanoparticles with NH<sub>2</sub> and SH groups. The Ag nanoparticles bound to the surfaces of the NH<sub>2</sub>-functionalized SiO<sub>2</sub> nanoparticles through coordinative bonds between the empty orbitals

**Table 1.** Experimental conditions employed for the preparation of heterogeneous Ag-SiO<sub>2</sub> nanocomposite particles

Sample	Functionalizing agent	Molecular weight of PVP	PVP concentration [wt%]	Average size of immobilized Ag NPs [nm]
# 01	APTMS	10,000	0.5	10
# 02	APTMS	29,000	0.5	7-8
# 03	APTMS	40,000	0.5	5-7
# 04	APTMS	58,000	0.5	5
# 05	APTMS	29,000	1	11-12
# 06	APTMS	29,000	1.5	14-15
# 07	APTMS	29,000	2.5	14-15
# 08	MPTMS	10,000	0.5	6-8
# 09	MPTMS	29,000	0.5	4-6
# 10	MPTMS	40,000	0.5	3-4
# 11	MPTMS	58,000	0.5	2-3
# 12	MPTMS	29,000	1	6-7
# 13	MPTMS	29,000	1.5	5-7
# 14	MPTMS	29,000	2.5	2-3

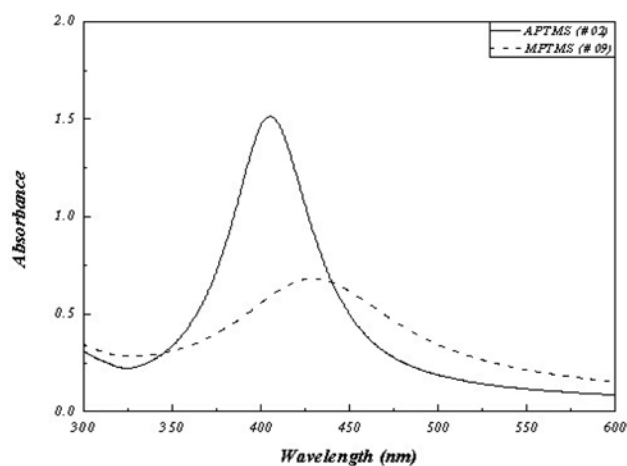
of the Ag atoms and the lone pair electrons of the N atoms. The Ag nanoparticles bound to SH-functionalized SiO<sub>2</sub> nanoparticles through cleavage of the S-H bonds and spontaneous formation of S-Ag bonds [15]. Fig. 1 displays TEM images of the nanocomposites obtained from the NH<sub>2</sub>-functionalized SiO<sub>2</sub> nanoparticles after performing immobilization of Ag nanoparticles. The average diameter of the Ag nanoparticles on the NH<sub>2</sub>-functionalized SiO<sub>2</sub> surface was ca. 10 nm. The Ag nanoparticles that formed on the SH-functionalized SiO<sub>2</sub> surface were relatively small and immobilized more densely.

Fig. 2 displays the UV-vis. spectra of the Ag-SiO<sub>2</sub> nanocomposites prepared from the NH<sub>2</sub>- and SH-functionalized SiO<sub>2</sub> nanoparticles (samples 02 and 09, respectively). The spectrum of the nanocomposite derived from the NH<sub>2</sub>-presenting SiO<sub>2</sub> surface featured a narrow absorbance peak. In contrast, the spectrum of the nanocomposite prepared from the SH-presenting SiO<sub>2</sub> nanoparticles exhibited a broad, red-shifted peak. The red-shifted peak suggested that this nanocomposite featured a greater coverage of Ag nanoparticles on the SiO<sub>2</sub> surface, consistent with our observations from the TEM images.

We selected PVP, which combines a hydrophobic polyvinyl backbone with hydrophilic pendent groups that interact with polar solvents, as a surfactant to prevent the Ag NPs from aggregating through steric effects [28]. Figs. 1 and 3 reveal the influence of the molecular weight of the PVP polymer on the resulting Ag-SiO<sub>2</sub> nanocomposites. The TEM images indicate that the average size of the Ag nanoparticles on the SiO<sub>2</sub> nanoparticles surfaces decreased

upon increasing the molecular weight of PVP. Because the monomer units in PVP contain imide groups, this polymer has many active sites to bind metal ions. This situation causes PVP to disperse the silver ions well, making it easier to immobilize the Ag nanoparticles onto the SiO<sub>2</sub> nanoparticle surfaces.

When we used PVP having a molecular weight of 10,000, there were more opportunities for seed growth because of the short polymer chain length. As a result, the average size of the Ag nanoparticles on the SiO<sub>2</sub> nanoparticles surfaces increased. Upon increasing the molecular weight of PVP, the physical barrier to seed



**Fig. 2.** UV-vis. spectra of Ag-SiO<sub>2</sub> nanocomposite particles prepared from NH<sub>2</sub>- and SH-functionalized SiO<sub>2</sub> nanoparticles.

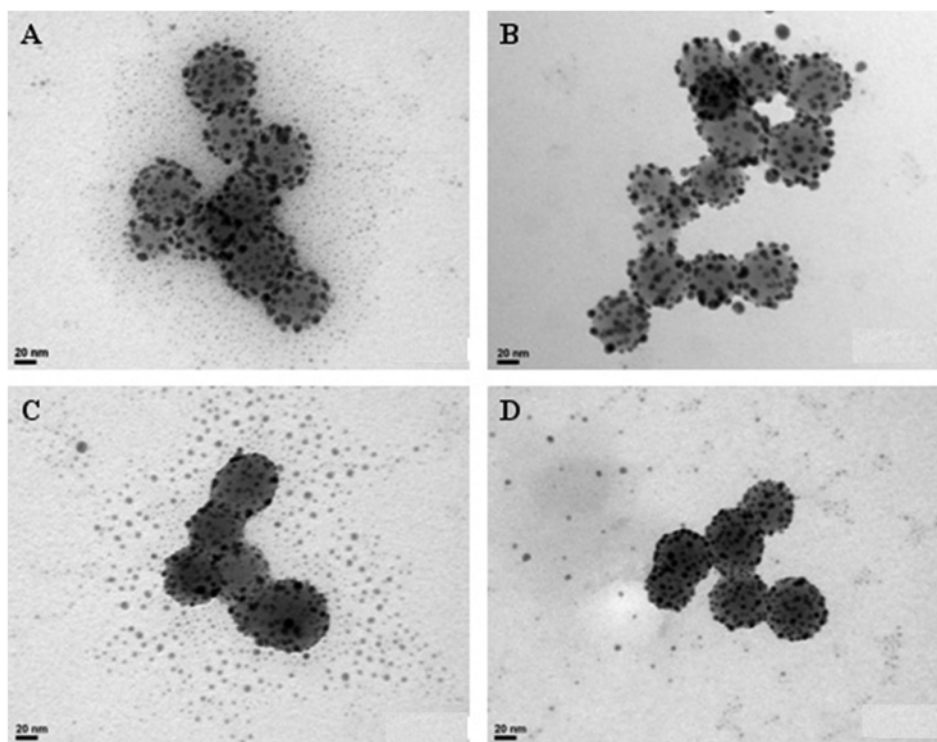


**Fig. 1.** TEM images of Ag-SiO<sub>2</sub> nanocomposite particles prepared from the NH<sub>2</sub>-functionalized SiO<sub>2</sub> nanoparticles in the presence of PVP polymers having different molecular weights (A: # 01, B: # 02, C: # 03, D: # 04).

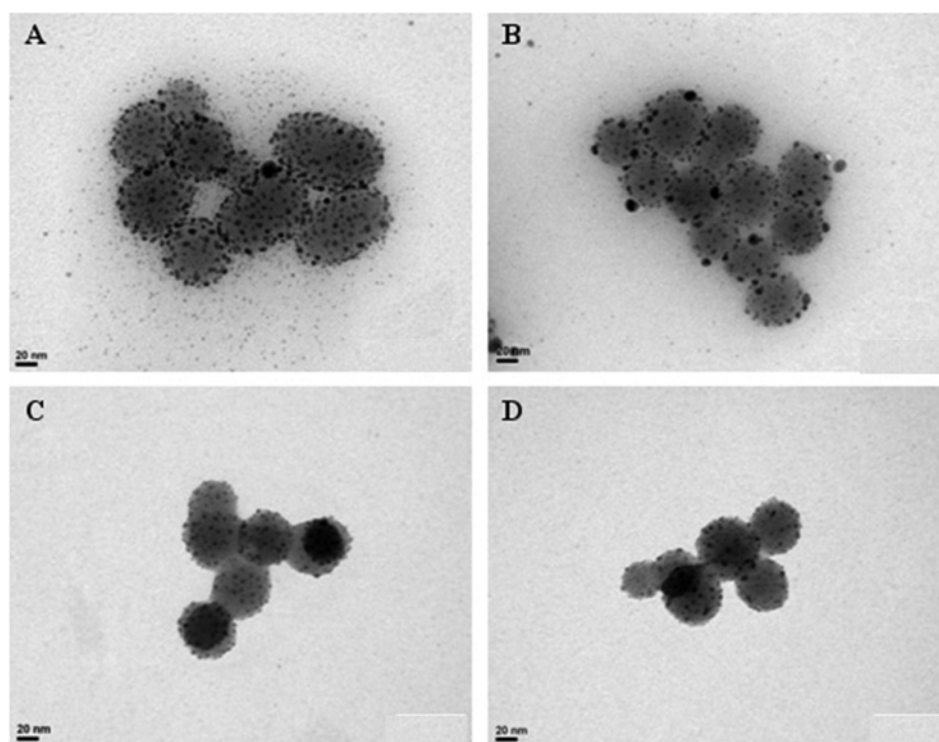


**Fig. 3.** TEM images of Ag-SiO<sub>2</sub> nanocomposite particles prepared from the SH-functionalized SiO<sub>2</sub> nanoparticles in the presence of PVP polymers having different molecular weights (A: # 08, B: # 09, C: # 10, D: # 11).

growth increased because of the steric effects of the long chain polymer and, therefore, the average size of the Ag nanoparticles decreased. This phenomenon occurred for the Ag-SiO<sub>2</sub> nanocomposites prepared from both the NH<sub>2</sub>- and SH-functionalized SiO<sub>2</sub> surfaces, but the number of immobilized Ag nanoparticles on the latter was greater and their average size was more monodisperse (Fig. 3).

Figs. 4 and 5 display UV-vis. spectra of the Ag-SiO<sub>2</sub> nanocomposites obtained from the NH<sub>2</sub>- and SH-functionalized SiO<sub>2</sub> nanoparticles, respectively, in the presence of PVP polymers having different molecular

weights. In both cases, increasing the molecular weight of PVP led to a decrease in the height of the absorbance signal, *i.e.*, a decrease in the average size of the Ag nanoparticles on the treated SiO<sub>2</sub> surfaces. When we used long chain PVPs (M.W. = 40,000 and 58,000), the absorbance signals were almost identical in each system.

In addition to playing an important role in protecting the synthesized particles, PVP also behaves as a reducing agent. In previous studies, we employed PVP to synthesize Ag and Pt nanoparticles using a modified version of the alcohol reducing process [26, 27]; we found that

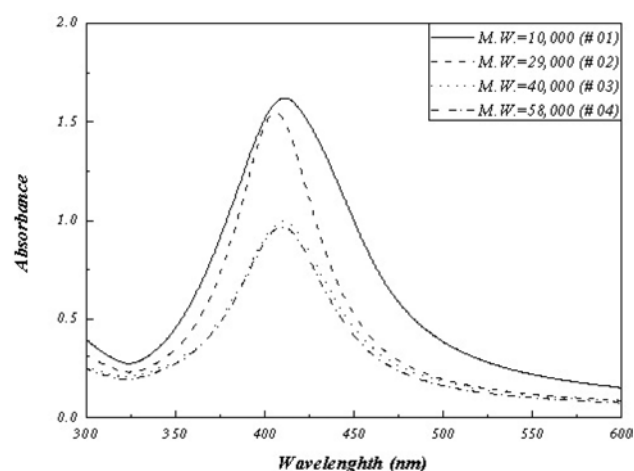


**Fig. 4.** UV-Vis spectra of Ag-SiO<sub>2</sub> nanocomposite particles prepared from the NH<sub>2</sub>-functionalized SiO<sub>2</sub> nanoparticles in the presence of PVP polymers having different molecular weights.

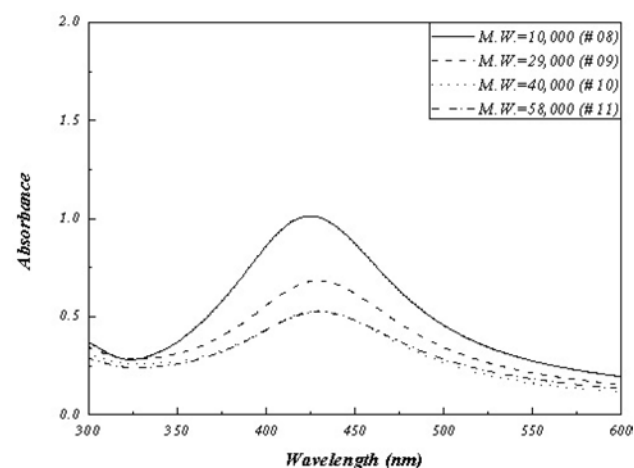


**Fig. 5.** UV-Vis spectra of Ag-SiO<sub>2</sub> nanocomposite particles prepared from the SH-functionalized SiO<sub>2</sub> nanoparticles in the presence of PVP polymers having different molecular weights.

the PVP concentration affected the rates of reduction of the metal ions, which determined their nanoparticles sizes. To gain a better insight into our present reactions, we studied the influence of the PVP concentration on the formation of the Ag-SiO<sub>2</sub> nanocomposites under the conditions outlined

in Table 1. Figs. 6 and 7 display TEM images of the Ag-SiO<sub>2</sub> nanocomposites prepared from the NH<sub>2</sub>- and SH-functionalized SiO<sub>2</sub> nanoparticles, respectively, in the presence of various concentrations of PVP. The average size of the Ag nanoparticles on the NH<sub>2</sub>-presenting SiO<sub>2</sub>

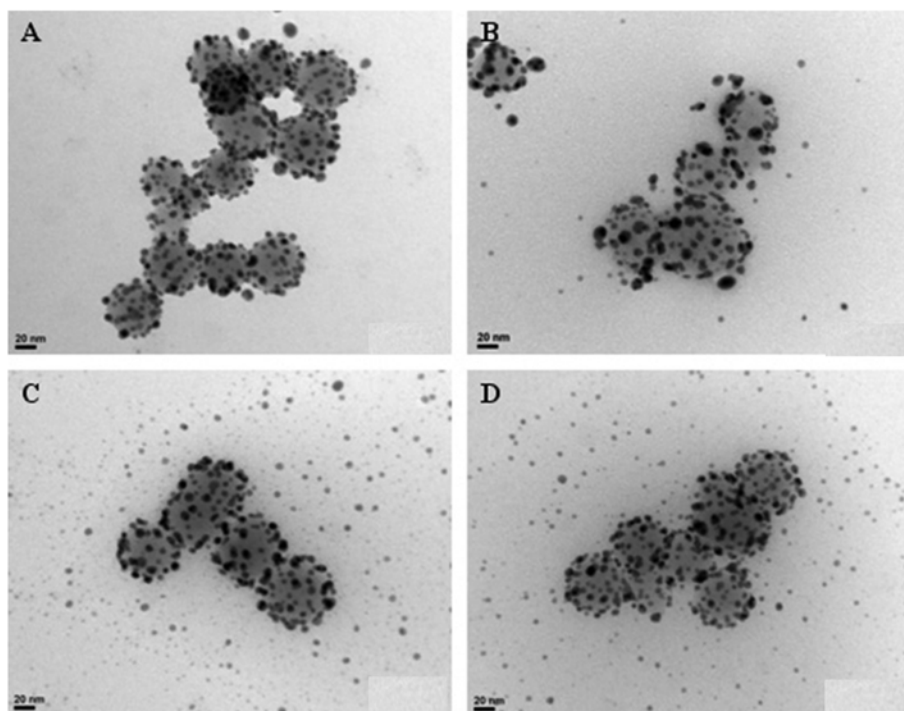


**Fig. 6.** TEM images of Ag-SiO<sub>2</sub> nanocomposite particles prepared from the NH<sub>2</sub>-functionalized SiO<sub>2</sub> nanoparticles in the presence of the PVP polymer (M. W. = 29,000) at various concentrations (A: # 02, B: # 05, C: # 06, D: # 07).

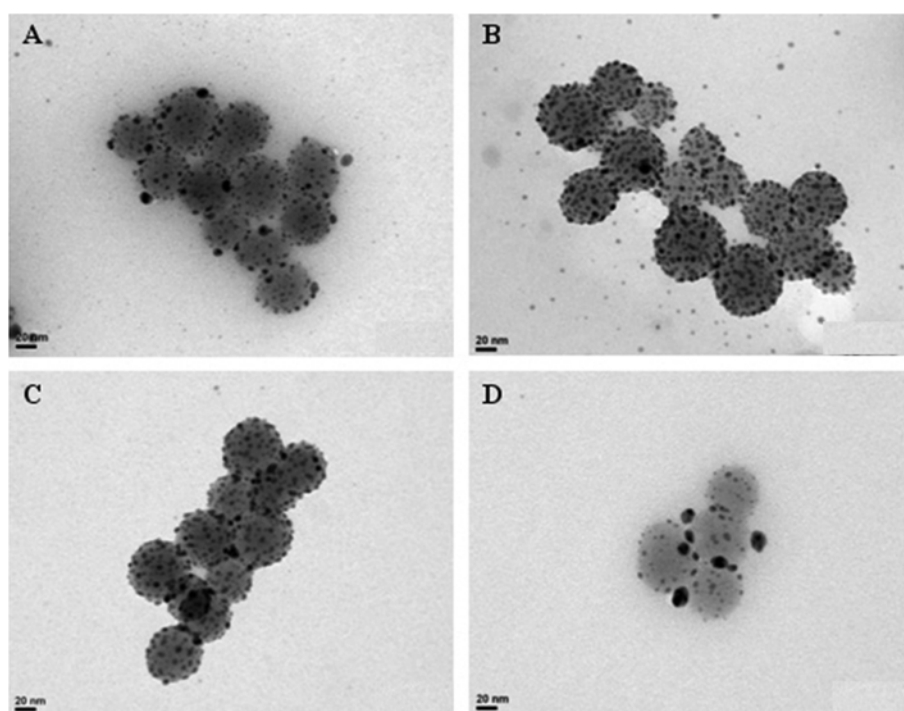


**Fig. 7.** TEM images of Ag-SiO<sub>2</sub> nanocomposite particles prepared from the SH-functionalized SiO<sub>2</sub> nanoparticles in the presence of the PVP polymer (M. W. = 29,000) at various concentrations (A: # 09, B: # 12, C: # 13, D: # 14).

surfaces increased upon increasing the PVP concentration. In addition, the number of free Ag nanoparticles, *i.e.*, those not immobilized on the treated SiO<sub>2</sub> nanoparticles, increased upon increasing the PVP concentration and free Ag particles. This behavior resulted from Ostwald ripening and steric effects. The effect of the PVP concentration remained unchanged when the concentration was 1.5 wt% or more.

In contrast, the PVP concentration did not affect the average size of the Ag-SiO<sub>2</sub> nanocomposites obtained from the SH-functionalized SiO<sub>2</sub> nanoparticles, although an increase in the PVP concentration decreased the number of free Ag nanoparticles (Fig. 7). When the PVP concentration was 1.5 wt% or more, almost no free Ag nanoparticles existed in the solution. When the PVP concentration was 2.5 wt%, the immobilized Ag nanoparticles were too large to adhere to the SiO<sub>2</sub> surface through Ag-S bonds. Consequently, several large immobilized Ag nanoparticles were cleaved from the surface of the treated SiO<sub>2</sub> NPs (Fig. 7(D)).

Figs. 8 and 9 present the UV-Vis spectra of the Ag-SiO<sub>2</sub> composites obtained from the NH<sub>2</sub>- and SH-functionalized SiO<sub>2</sub> nanoparticles, respectively, in the presence of various PVP concentrations. In both cases, an increase in the PVP concentration increased the height of the absorbance, *i.e.*, it increased the average size of the Ag nanoparticles on the treated SiO<sub>2</sub> surfaces, except that the peak from the Ag-SiO<sub>2</sub> nano-composites prepared from the SH-functionalized SiO<sub>2</sub> was more intense when the PVP concentration was 1.5 wt% than when it was 2.5 wt%. The spectra of the Ag-SiO<sub>2</sub> nanocomposites prepared from the NH<sub>2</sub>-presenting SiO<sub>2</sub> nanoparticles featured narrower and taller absorbance peaks than those prepared from the SH-presenting SiO<sub>2</sub> surfaces.

## Conclusions

We have used an alcohol reducing method of AgNO<sub>3</sub> to prepare heterogeneous Ag-SiO<sub>2</sub> nanocomposites from

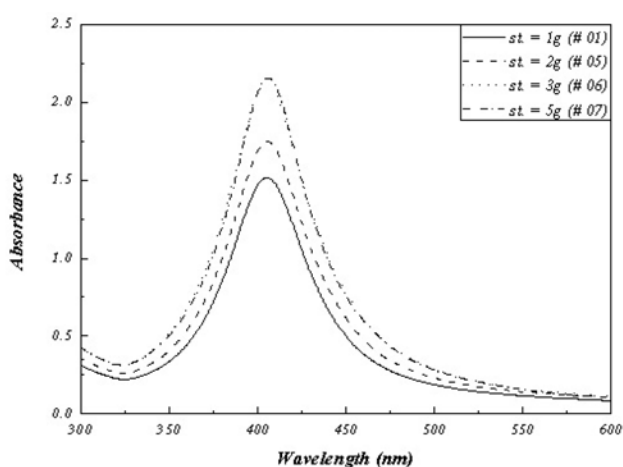


**Fig. 8.** UV-Vis spectra of Ag-SiO<sub>2</sub> nanocomposite particles prepared from the NH<sub>2</sub>-functionalized SiO<sub>2</sub> nanoparticles in the presence of the PVP polymer (M. W. = 29,000) at various concentrations.

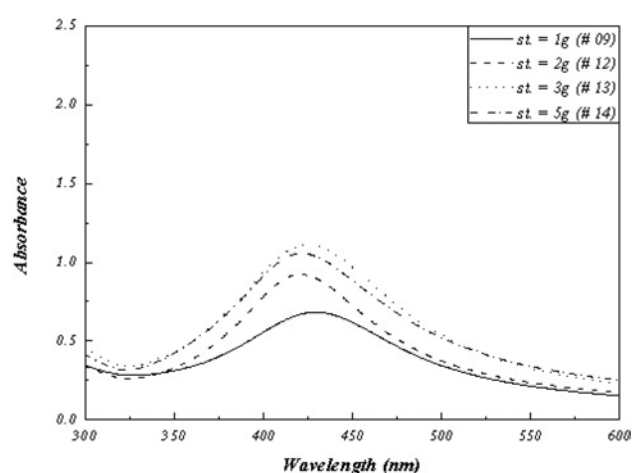


**Fig. 9.** UV-Vis spectra of Ag-SiO<sub>2</sub> nanocomposite particles prepared from the SH-functionalized SiO<sub>2</sub> nanoparticles in the presence of the PVP polymer (M. W. = 29,000) at various concentrations.

SiO<sub>2</sub> nanoparticles presenting NH<sub>2</sub> and SH functional groups on their surfaces. In general, the Ag nanoparticles immobilized on the surfaces of the SiO<sub>2</sub> nanoparticles had an average diameter of ca. 15 nm. Both the concentration and molecular weight of the PVP added affected the rate of reduction of the Ag<sup>+</sup> ions, which determined the size of the resulting Ag nanoparticles. The average Ag nanoparticle size increased upon increasing the concentrations of PVP.

## Acknowledgment

This study was supported by the research fund of Hanyang University (HY-2007-I).

## References

1. Y. Kobayashi, V. Salgueirinho-Maceira and L.M. Liz-Marzan, *Chem. Mater.* 13 (2001) 1630-1633.
2. R. Blonder, L. Sheeney and I. Willner, *Chem. Commun.* (1998) 1393-1394.
3. M. Haneda, Y. Kintaichi, M. Inaba and H. Hamada, *Catal. Today* 42 (1998) 127-135.
4. S.-W. Kim, M. Kim, W.Y. Lee and T. Hyeon, *J. Am. Chem. Soc.* 124 (2002) 7642-7643.
5. L. Lu, G. Sun, S. Xi, H. Wang and H. Zhang, *Langmuir* 19 (2003) 3074-3077.
6. Y. Zhou, C.Y. Wang, H.J. Liu, Y.R. Zhu and Z.Y. Chen, *Mater. Sci. Eng.* B67 (1999) 95-98.
7. L. Zhang, J.C. Yu, H.Y. Yip, Q. Li, K.W. Kwong, A.-W. Xu and P.K. Wong, *Langmuir* 19 (2003) 10372-10380.
8. C.W. Chen, T. Serizawa and M. Akashi, *Polym. Adv. Technol.* 10 (1999) 127-133.
9. S. Tang, Y. Tang, S. Zhu, H. Lu and X. Meng, *J. Solid State Chem.* 180 (2007) 2871-2876.
10. M.W. Zhu, G.D. Qian, Z.L. Hong, Z.Y. Wang, X.P. Fan and M.Q. Wang, *J. Phys. Chem. Solid.* 66 (2005) 748-752.
11. C. Graf and A. van Blaaderen, *Langmuir* 18 (2002) 524-534.
12. R.L. Moody, T. Vo-Dinh and W.H. Fletcher, *Appl. Spectrosc.*

- 41 (1987) 966-972.
13. T. Cassagneau and F. Caruso, *Adv. Mater.* 14 (2002) 732-736.
  14. V.G. Pol, D.N. Srivastava, O. Palchik, V. Palchik, M.A. Slifkin, A.M. Weiss and A. Gedanken, *Langmuir* 18 (2002) 3352-3357.
  15. J.-M. Lee, D.-W. Kim, Y.-D. Jun and S.-G. Oh, *Mater. Res. Bull.* 41 (2006) 1407-1416.
  16. Y.T. Lim, O.O. Park and H.-T. Jung, *J. Colloid Interface Sci.* 263 (2003) 449-453.
  17. A.P. Philipse and A. Vrij, *J. Colloid Interface Sci.* 128 (1989), 121-136.
  18. N.L. Dias Filho, Y. Gushikem and W.L. Polito, *Anal. Chem. Acta* 306 (1995) 167-172.
  19. C. Kantipuly, S. Katragadda, A. Chow and H.D. Gesser, *Talanta* 37 (1990) 491-517.
  20. L. Mercier and T. J. Pinnavaia, *Adv. Mater.* 9 (1997) 500-503.
  21. X. Feng, G.E. Fryxell, L.Q. Wang, A.Y. Kim, J. Liu and K.M. Kemner, *Science* 276 (1997) 923-926.
  22. L. Mercier and T.J. Pinnavaia, *Environ. Sci. Technol.* 32 (1998) 2749-2754.
  23. P.N. Floriano, O. Schlieben, E.E. Doomes, I. Klein, J. Janssen, J. Hormes, E.D. Poliakov and R.L. McCarley, *Chem. Phys. Lett.* 321 (2000) 175-181.
  24. S.J. Oldenburg, R.D. Averitt, S.L. Westcott and N.J. Halas, *Chem. Phys. Lett.* 288 (1998) 243-247.
  25. T. Pham, J.B. Jackson, N.J. Halas and T.R. Lee, *Langmuir* 18 (2002) 4915-4920.
  26. C.Y. Kim, S.H. Jeong and S.C. Yi, *J. Ceram. Process. Res.* 8 (2007) 445-449.
  27. C.Y. Kim, B.M. Kim, S.H. Jeong and S.C. Yi, *J. Ceram. Process. Res.* 7 (2006) 241-244.
  28. Z. Zhang, B.-Z. and L. Hu, *J. Solid State Chem.* 121 (1996) 105-110.